NASA Contractor Report 4004

A Fundamental Study of Drag and an Assessment of Conventional Drag-Due-to-Lift Reduction Devices

John E. Yates and Coleman duP. Donaldson

CONTRACT NAS1-18065
SEPTEMBER 1986

NASA

NASA Contractor Report 4004

A Fundamental Study of Drag and an Assessment of Conventional Drag-Due-to-Lift Reduction Devices

John E. Yates and Coleman duP. Donaldson
Aeronautical Research Associates of Princeton, Inc.
Princeton, New Jersey

Prepared for
Langley Research Center
under Contract NAS1-18065

National Aeronautics
and Space Administration

**Scientific and Technical
Information Branch**

1986

TABLE OF CONTENTS

SUMMARY

The theory of drag and lift is revisited starting with the integral conservation laws of fluid mechanics. Many representations (some known and some unknown) of drag and lift are derived in terms of far wake properties, intermediate wake properties and surface loading. Although the theoretical results are quite general, these representations are used in the present report primarily to assess the drag efficiency of lifting wings both CTOL and various out-of-plane configurations.

The drag-due-to-lift is separated into two major components that reveal themselves quite naturally in the theory. The first and largest component is the "induced" drag-due-to-lift that is due to spanwise variations of wing loading. It is a strong function of aspect ratio for a CTOL wing or more generally the projection of the lifting elements on the Trefftz plane. The first component is relatively independent of Reynolds number or details of the wing section design or planform. For each lifting configuration there is an optimal load distribution that yields the minimum value of drag-due-to-lift against which the efficiency of a particular design may be assessed. The second and much smaller component of drag-due-to-lift may be called "form" drag-due-to-lift. It is largely independent of aspect ratio but strongly dependent on the details of the wing section design, planform and Reynolds number. It is a result of wing load variations in the chordwise direction.

For well designed high aspect ratio CTOL wings the two drag components are to lowest order independent with only a weak interaction of the order of the square of the drag coefficient (i.e., a percent or so of wing drag). With modern design technology CTOL wings can be (and usually are) designed with a drag-due-to-lift efficiency close to unity. Wing tip-devices (winglets, feathers, sails, etc.) that have vertical dimensions of the order of the wing chord can probably improve drag-due-to-lift efficiency by 10 or 15% if they are designed as an integral part of the wing with the proper load on all lifting elements. As add-on devices for a well designed CTOL wing they can be detrimental. The largest increments of drag-due-to-lift efficiency can be attained with joined tip configurations and vertically separated lifting elements. It is estimated that 25% improvements of wing drag efficiency can be obtained without considering additional benefits that might be realized by improved structural efficiency. It is strongly recommended that an integrated aerodynamic/structural approach be taken in the design of or research on future out-of-plane configuration.

1. INTRODUCTION

The resistance of bodies moving in a fluid medium (drag) is a subject of considerable interest to the aircraft designer so much so that regular symposia (national and international) are held to discuss the efficiency of modern designs and exchange ideas on the relative merits of various drag reducing devices (see Ref. 1, e.g.). For the modern CTOL airplane there is almost equal partition of the total drag into form drag and drag-due-to-lift. Drag research is usually focused on one or the other of these topics. Recent efforts on the development of laminar flow airfoils (Ref. 1, papers of Saric or Braslow and Fischer) and riblets (Ref. 1, paper by Bushnell) to reduce turbulent skin friction are primarily concerned with the reduction of form drag. We will see herein that a reduction of form drag (at least on a lifting surface) also has a secondary benefit of reducing the drag-due-to-lift.

Research efforts on drag-due-to-lift have focused primarily on improved wing efficiency. Planform optimization (in particular the tip design) has held the center of attention (Ref. 2) since the advent of the Whitcomb winglet (Ref. 3). Many devices both active and inactive have been proposed (Refs. 4,5,6 & 7) as drag-due-to-lift reduction devices and many claims have been made about the ability of these devices to reduce drag. The purpose of this study is to assess these claims rationally and to pinpoint those areas of research that could have the biggest payoff for both current CTOL and future aircraft designs. The underlying theoretical principles that are absolutely essential for attempting such a project are developed in Section 2. Much of the theoretical discussion may sound familiar to the reader but to our knowledge many of the theoretical relations between drag and wake vorticity are fundamentally new. Also, the most important principle to be gleaned from the multitude of theoretical formulas is the generalization of the notion of an optimal drag-due-to-lift for a given configuration. This idea has been around since the development of lifting line theory although the "optimal result" is often criticized because it is based on a linear theory. It must be understood that the idea follows directly from the global conservation principles of fluid mechanics revisited in Section 2. There is in a sense a "Carnot Drag Efficiency" for a given lifting configuration whether it be the CTOL wing, bi-wing, box-wing, a wing with winglets or what have you. It is against this optimal efficiency that we assess the various drag reduction devices in Section 3.

Finally we remark that the general theory can be used to unify and provide more rational definitions of some of the traditional drag components. For example, it is customary to consider the wing tip shape to have an influence on the drag-due-to-lift or in particular the "induced drag." On the other hand the drag associated with the wing-fuselage junction is termed "interference drag" and a whole new set of design principles have evolved to combat this drag component when in fact it is fundamentally of the same origin as induced drag; i.e., variation of the load in the cross stream direction with the production of strong axial vorticity. With a more unified viewpoint the emphasis on wing tip design can perhaps be put into better perspective as only one component of a totally integrated design both aerodynamic and structural. The biggest payoff in the future may well be in the design of

configurations that eliminate all unnecessary cross stream load variations (a strong case for the flying wing and joined tip configuration) in particular if there are structural benefits to be realized.

In this study we have deliberately omitted any detailed considerations or evaluation of active devices such as tip blowing, propellers, etc. The lifting configurations of this study do not exchange mass, momentum or energy at their boundary so that drag efficiency can be measured in terms of entropy production of the airframe for a required amount of lift. If part of the powerplant energy or auxiliary energy is used to alter the flow over the lifting elements then the drag becomes difficult if not impossible to separate from the powered thrust. Efficiency must then be measured in terms of total power requirements (including all auxiliary blowing) for a given lift. While this can and must be done to evaluate active devices we have concentrated on the efficiency of inactive lifting elements herein. A natural and worthwhile follow on to the present study would be to revise the basic formulation of Section 2 to include mass, momentum and energy exchange at all surfaces and so integrate the powerplant and auxiliary blowing devices into the aerodynamic evaluation.

NOMENCLATURE

A	b^2/S, aspect ratio (or angular momentum in half control volume)
b	wing span
c(y)	chord distribution of wing planform
$c_d(y)$	section drag distribution
$c^*_{d_s}$	average wing section drag coefficient
c_f	flat plate skin friction coefficient
$c_{\ell\alpha}$	section lift curve slope
C_D	$D/S \cdot q_\infty$, drag coefficient based on area S of lifting surface
C_{D_i}	drag associated with wake cross flow kinetic energy (induced drag-due-to-lift) see (2.3.28)
C_{D_0}	drag in absence of lift
C_L	$L/S \cdot q_\infty$, lift coefficient
C_{L_α}	total lift curve slope
D	$\vec{i} \cdot \vec{F}$, drag, see (2.1.4) and (2.1.6)
e	energy/unit mass (or wing efficient factor, see (2.3.31))
E	total energy in control volume see (2.1.1)
f(x,y)	wing thickness distribution, see (2.4.3)
$\vec{F}$	resultant force, see (2.1.4)
g(x,y)	wing camber and twist distribution, see (2.4.3)
H	$h+v^2/2$, total enthalpy
k	section drag-due-to-lift factor, see (2.4.17 and 2.4.18)
K	wing total drag-due-to-lift factor, see (2.4.15 and 2.4.16)
K_f	form drag-due-to-lift factor, see (4.2.)
K_i	induced drag-due-to-lift factor, see (4.2)
L	lift, see (2.1.4 and 2.1.5)

ℓ_o integral scale of wake vorticity, see (2.3.27)

ℓ_s fraction of wing leading edge that is separated, see (2.5.5)

M total mass in control volume see (2.1.1)

M_∞ Mach number at infinity

p static fluid pressure

P $p+\rho\ v^2/2$, total head pressure

$\vec{P}$ total momentum in control volume, see (2.1.1)

$\vec{q}$ heat flux vector

R gas constant, see (2.2.1)

R_e Reynolds number

s entropy/unit mass

$\mathscr{S}$ total entropy in control volume, see (2.1.)

S reference area of wing

t time

T Trefftz plane (or temperature)

$T_{1/2}$ half Trefftz plane

u_∞ free stream velocity in x-direction, see Figure 2.1

v_n normal component of velocity on a surface with normal $\vec{n}$

$\vec{v}$ (u,v,w) velocity components

v magnitude of velocity in the Trefftz plane

w_{av} average circulation velocity, see (2.4.24)

$\vec{x}$ (x,y,z) cartesian coordinates, see Figure 2.1

$\bar{y}$ vortex span, see (2.3.4)

α angle of attack (geometric)

δ measure of wing max camber or twist

δ_w^* wake displacement thickness, see (2.5.9)

Δ	difference pressure coefficient or load, see (2.4.5)
Δs	$s-s_\infty$
ε	measure of wing max thickness
γ	ratio of specific heats, see (2.2.1)
$\Gamma(r)$	circulation distribution in wake
Γ_0	total vorticity (circulation) in half Trefftz plane see (2.3.3)
λ_s	see (2.5.4)
μ	fluid viscosity
ρ	mass density
ρ_∞	free stream density
σ	mean pressure coefficient, see (2.4.4)
$\vec{\vec{\tau}}$	viscous stress tensor
$\vec{\psi}$	stream function, see (2.3.13)
$\vec{\omega}$	curl $\vec{v}$, vorticity

2. FUNDAMENTAL THEORY

2.1 Integral Conservation Laws

Consider a lifting body (airplane) fixed in a fluid that moves in the positive x direction at speed u_∞ as shown in Figure 2.1. We further consider a cylindrical control volume V that encloses the body and is bounded by an upstream y-z plane T_∞ and a downstream (Trefftz) plane T at an arbitrary location x. The cylindrical boundary is denoted by C and the surface of the airplane by S. Also $\vec{n}$ is the unit normal on the outer boundary (positive out of V) and on S (positive into V). We consider the conservation of mass, linear and angular momentum, energy and entropy (also total head) and their relation to the resultant force that acts on the airplane:

$$M = \int_V \rho dV \qquad \text{Mass}$$

$$\vec{P} = \int_V \rho\vec{v}dV \qquad \text{Linear Momentum}$$

$$A = \int_{V_{1/2}} \vec{i}\cdot\vec{x}\times\rho\vec{v}dV \qquad \text{Angular Momentum (Half Control Volume)}$$

$$E = \int_V \rho(e+v^2/2)dV \qquad \text{Energy}$$

$$\mathscr{S} = \int_V \rho s dV \qquad \text{Entropy} \qquad (2.1.1)$$

The compressible viscous equations of fluid motion are:

$$\frac{\partial\rho}{\partial t} + \text{div}\ \rho\vec{v} = 0$$

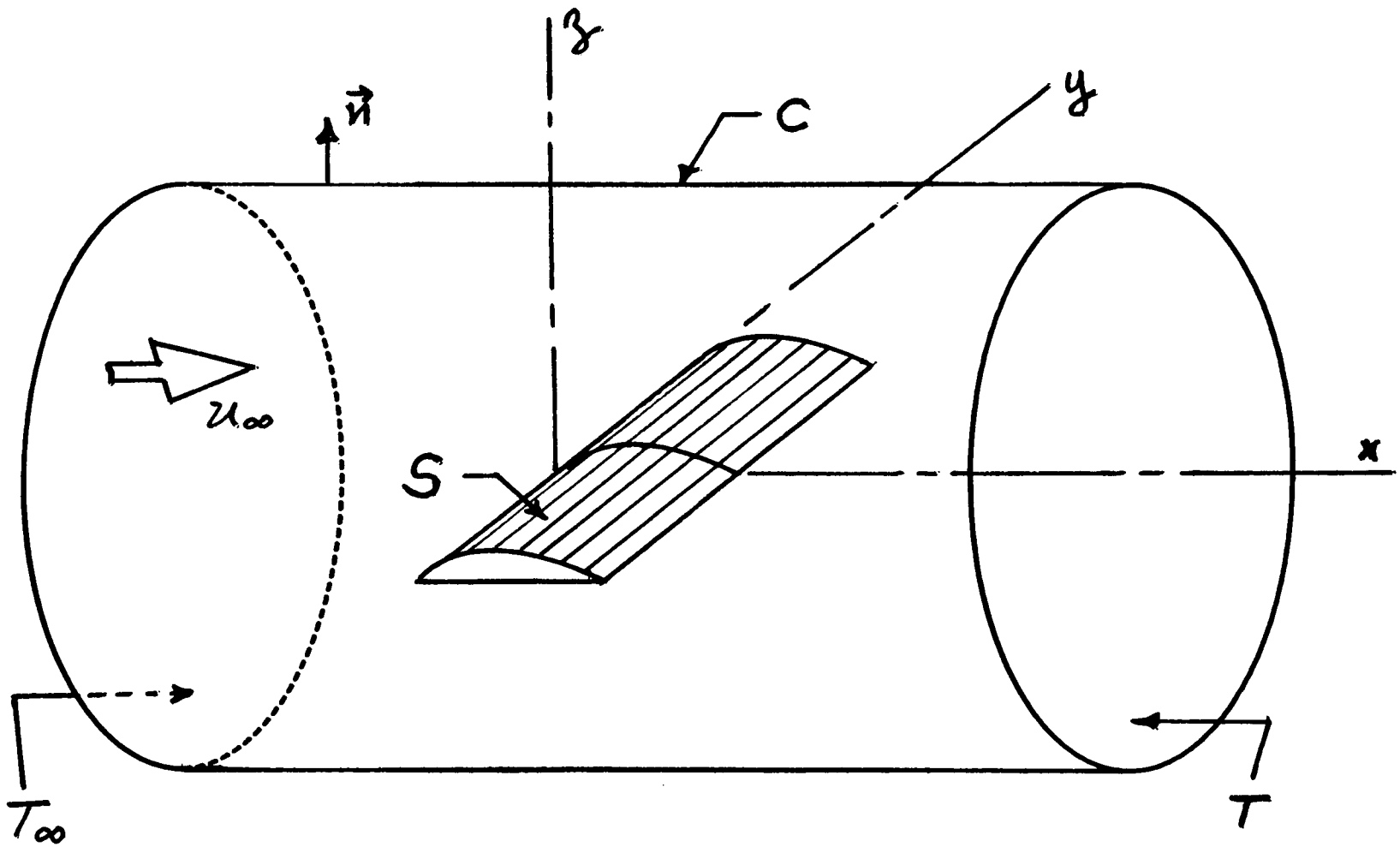

Figure 2.1 - Lifting Configuration in a Control Volume, V.

$$\frac{\partial \rho \vec{v}}{\partial t} + \text{div}\ (\rho \vec{v}\vec{v} + p\ \vec{\vec{I}} - \vec{\vec{\tau}}) = 0$$

$$\frac{\partial}{\partial t}\ \rho(e+v^2/2) + \text{div}\left[\rho \vec{v}(e+v^2/2) + p\vec{v} - \vec{\vec{\tau}}\cdot\vec{v} + \vec{q}\right] = 0 \qquad (2.1.2)$$

We compute the time rate of change of each of the global quantities defined in (2.1.1) and assume that in steady state operation the time average rate of change is zero. The time average of all subsequent equations is implied although we have omitted any explicit notation to indicate averages. We assume that the velocity and heat flux through S are zero. Also we assume that the Reynolds number is very large so that contributions of viscous stresses on the outer control boundary may sensibly be neglected. The conservation of mass leads to the following integral equation for the outflow through C and T,

$$\rho_\infty \int_C v_n dS = \int_T (\rho_\infty u_\infty - \rho u) dS \qquad (2.1.3)$$

a result that is used in all subsequent equations. The conservation of linear momentum leads to the following representation of the resultant force on S:

$$\vec{F} \equiv -\int_S (p\vec{n} - \vec{\vec{\tau}}\cdot\vec{n})dS \qquad \text{Resultant Force}$$

$$= \vec{i}D + \vec{L} \qquad \text{with} \qquad \vec{i}\cdot\vec{L} = 0 \qquad (2.1.4)$$

where D is the total drag due to pressure and viscous stresses and by definition is the projection of the resultant force on the free stream direction. The transverse force is denoted by $\vec{L}$ and if the x-z plane is a plane of symmetry, then $\vec{L} = \vec{k}L$ where L is the lift. We assume a plane of symmetry in the following development. The Trefftz plane representations of the lift and drag are given by

$$L = -\int_T \rho u w dS \qquad \text{Lift} \tag{2.1.5}$$

$$D = \int_T [p_\infty - p + \rho u(u_\infty - u)] dS \qquad \text{Drag} \tag{2.1.6}$$

while the surface definitions of lift and drag are given by

$$L \equiv -\int_S (p\,\vec{k}\cdot\vec{n} - \vec{k}\cdot\vec{\tau}\cdot\vec{n}) dS \tag{2.1.7}$$

$$D \equiv -\int_S (p\,\vec{i}\cdot\vec{n} - \vec{i}\cdot\vec{\tau}\cdot\vec{n}) dS \tag{2.1.8}$$

The conservation of angular momentum in one half of the control volume leads to an expression for the root bending moment; i.e.,

$$M = \int_{T_{1/2}} \rho u\, \vec{i}\cdot(\vec{x}\times\vec{v}) dS + \underbrace{\int_{y=0}}_{\substack{\text{Symmetry} \\ \text{plane}}} (p - \rho_\infty)\cdot z\, dx dz \tag{2.1.9}$$

while M is defined in terms of surface forces by

$$M = -\int_{S_{1/2}} dS[\vec{i}\cdot\vec{x}\times\vec{n}p - \vec{i}\cdot\vec{x}(\vec{\tau}\cdot\vec{n})] \tag{2.1.10}$$

where the subscript (1/2) denotes one half of the wing, the Trefftz plane or control volume bounded by the symmetry plane y = 0.

The conservation of total energy combined with the assumption of an adiabatic surface S leads to the conclusion that the total enthalpy deficit in the Trefftz plane is zero; i.e.,

$$\int_T \rho u(H_\infty - H)dS = 0 \qquad (2.1.11)$$

where

$$H = h + v^2/2 \qquad \text{(Total Enthalpy)} \qquad (2.1.12)$$

Conservation of entropy combined with Fourier's law of internal heat conduction leads to the following result for entropy flux through the Trefftz plane:

$$\int_T \rho u(s - s_\infty)dS = \int_V \left[\mu \left(\frac{\vec{\tau} \cdot \text{grad } \vec{v}}{T \cdot \mu} \right) + k \left(\frac{\text{grad} T}{T} \right)^2 \right] dV \geq 0 \qquad (2.1.13)$$

We remark that if the fluid is incompressible the last statement can be rewritten as a flux of total head loss; i.e.,

$$\int_T u(P_\infty - P)dS = \mu \int_V |\vec{\omega}|^2 \, dV \geq 0 \qquad (2.1.14)$$

where

$$P = p + \rho v^2/2 \qquad \text{(Total Head)} \qquad (2.1.15)$$

and $\vec{\omega} = \text{curl} \vec{v}$ is the vorticity.

2.2 Trefftz Plane Representations of the Drag and Lift

The objective of this section is to use the global conservation laws in conjunction with other principles of wing theory, Betz type wake roll-up theory, etc. to derive a variety of representations of the drag and lift from which solid conclusions can be drawn and which can be used to assess proposed methods for reducing drag, in particular drag-due-to-lift of conventional take off and land (CTOL) aircraft.

First we consider the fundamental Trefftz plane relation for the drag (2.1.6) and introduce the following perfect gas relations:

$$\frac{p}{p_\infty} = \left(\frac{h}{h_\infty}\right)^{\frac{\gamma}{\gamma-1}} e^{-\Delta s/R}$$

$$\frac{\rho}{\rho_\infty} = \left(\frac{h}{h_\infty}\right)^{\frac{1}{\gamma-1}} e^{-\Delta s/R} \qquad (2.2.1)$$

and assume that total enthalply is conserved on every streamline through the Trefftz plane. This is an assumption consistent with the global conservation of total enthalpy (2.1.11). We also note that total enthalpy is conserved across shock waves and adiabatic boundary layers (at least for unit Prandtl number), so that the assumption does not seem very severe. We further assume that in the Trefftz plane.

$$\frac{u_\infty - u}{a_\infty} << 1$$

$$v/a_\infty << 1$$

$$\Delta s/R << 1 \qquad (2.2.2)$$

With the foregoing assumptions, we obtain the following expression for the drag

$$D \cong \rho_\infty \int_T dS \left[\frac{a_\infty^2 \Delta S}{\gamma R} + \frac{v_I^2}{2} - (1-M_\infty^2) \frac{(u_\infty - u)^2}{2} \right] \qquad (2.2.3)$$

Another useful expression for the drag can be obtained if we introduce the definition of total head

$$P = p + \frac{\rho v_I^2}{2} + \frac{\rho u^2}{2} \tag{2.2.4}$$

The drag formula is

$$D = \int_T dS \left[P_\infty - P + \frac{\rho v_I^2}{2} - \frac{\rho (u_\infty - u)^2}{2} \right] \tag{2.2.5}$$

where the entropy rise in (2.2.3) has been replaced by total head loss in (2.2.5).

With the incompressible expression for total head flux (2.1.14) we can derive yet another drag formula

$$D = \frac{\mu}{u_\infty} \int_V |\vec{\omega}|^2 dV + \int_T \left[\frac{\rho v_I^2}{2} - \frac{\rho (u_\infty - u)^2}{2} + \left(1 - \frac{u}{u_\infty} \right) (P_\infty - P) \right] dS \tag{2.2.6}$$

We remark that a similar but somewhat messier expression can be obtained for compressible flow when the expression (2.1.13) for the entropy flux is substituted into (2.2.3).

Several important conclusions can be drawn from the above integral expressions. First we note that the streamwise location of the Trefftz plane is arbitrary. Thus we can differentiate (2.2.6) with respect to x. Since the drag is independent of x, we get

$$\frac{d}{dx} \int_T \left[\frac{\rho v_I^2}{2} - \rho \frac{(u_\infty - u)^2}{2} + \left(1 - \frac{u}{u_\infty} \right) (P_\infty - P) \right] dS$$

$$= - \frac{\mu}{u_\infty} \int_T |\vec{\omega}|^2 \, dV \quad \leq 0 \tag{2.2.7}$$

Thus the kinetic energy of the wake cross flow decays in proportion to the local enstrophy (both mean and turbulent) at station x. Both theoretical estimates and observations indicate that several miles are required for wake decay. Thus the kinetic energy and the total head loss are more or less

constant (adiabatic invariants) for many spans behind a high Reynolds number CTOL aircraft. This conclusion is in fact the justification for a Trefftz plane representation of classical induced drag and the conservation principles that underly the Betz wake roll-up theory.

Since all kinetic energy integrals over the Trefftz plane vanish as x tends to infinity we can write three equivalent expressions for the drag:

$$D = \lim_{x\to\infty} \int_T \rho_\infty a_\infty^2 \frac{\Delta s}{\gamma R}\, dS$$

$$= \lim_{x\to\infty} \int_T (P_\infty - P)\, dS$$

$$= \lim_{x\to\infty} \int_V \frac{\mu |\vec{\omega}|^2}{u_\infty}\, dV \qquad (2.2.8)$$

Conclusion:

All drag, by whatever name we may attach to it, is ultimately realized as an entropy rise or total head loss in the far wake. Also it is proportional to the volume integral of the squared vorticity (enstrophy). For an inviscid non-conducting fluid the drag is zero.

Next we introduce an approximation that can be justified for high aspect ratio CTOL aircraft. We omit details of the theoretical argument and resort to the following heuristic approach. Compare the drag given by (2.1.6) and (2.2.5). A major component of the drag ala (2.1.6) is due to the momentum deficit $(u_\infty - u)$ and in particular the profile drag (in absence of lift)

$$C_{D_0} \cong \frac{D_0}{S \cdot q_\infty} \cong \int_T \frac{dS}{S} \frac{u}{u_\infty} \left(1 - \frac{u}{u_\infty}\right)$$

$$= \int_T \frac{dS}{S} \left(1 - \frac{u}{u_\infty}\right) - \int_T \frac{dS}{S} \left(1 - \frac{u}{u_\infty}\right)^2 \qquad (2.2.9)$$

The profile drag coefficient is of order (.01) or less and for a "good" wing is primarily due to the linear term in (2.2.7). It seems plausible that we can argue that the quadratic term is of order (10^{-4}) or a few counts of drag coefficient. From an aircraft operational standpoint a few counts of drag is not negligible. However it is safe to say that neither the present theory or any proposed theory, CFD or laboratory experiment can claim 1% accuracy at least in the near future. For this reason we omit all terms in the analysis that are of the order of the drag coefficient squared and thus all terms that are quadratic in the axial momentum defect. The resulting approximate drag formulas are summarized below:

$$D = \int_T \left(\frac{\rho v_I^2}{2} + P_\infty - P \right) dS$$

$$= \int_T \frac{\rho v_I^2}{2} dS + \frac{\mu}{u_\infty} \int_V |\vec{\omega}|^2 dV \qquad (2.2.10)$$

Also we have the following auxiliary relations that follow from (2.1.6):

$$\int_T (P_\infty - P) dS \quad \int_T \rho u_\infty (u_\infty - u) dS$$

$$= \frac{\mu}{u_\infty} \int_V |\vec{\omega}|^2 dV \qquad (2.2.11)$$

and

$$\int_T (p_\infty - p) dS = \int_T \frac{\rho v_I^2}{2} dS \qquad (2.2.12)$$

It is consistent with these formulae to write the lift (2.1.5) and root bending moment (2.1.9) in the linearized forms

$$L = -\rho_\infty u_\infty \int_T w dS \qquad (2.2.13)$$

and

$$M = \rho_\infty u_\infty \int_{T_{1/2}} \vec{i}\cdot(\vec{x}x\vec{v})dS + \int_{y=0} (p-p_\infty)\cdot z \, dxdy \qquad (2.2.14)$$

2.3 Drag and Lift in Terms of Vorticity

The importance of vorticity in the representation and understanding of the origin of drag and lift cannot be overemphasized. We have already noted that the drag can be expressed in terms of the volume integral over all space of the squared vorticity. In this section we reduce the various drag and lift formulae derived above to integral moments and correlations of vorticity in the Trefftz plane. The relations so obtained form the basis for a large part of the accumulated practical understanding of drag-due-to-lift.

First we consider linear moments of vorticity in the Trefftz plane with the following definitions:

$$\omega_x = \frac{\partial w}{\partial y} - \frac{\partial v}{\partial z}$$

$$\omega_y = \frac{\partial u}{\partial z} - \frac{\partial w}{\partial x}$$

$$\omega_z = \frac{\partial v}{\partial x} - \frac{\partial u}{\partial y} \qquad (2.3.1)$$

The integral of ω_x, ω_y or ω_z over the entire Trefftz plane is zero. Thus we consider the linear moments. For example

$$\int_T dS \; y\omega_x = -\int_T w dS = \frac{L}{\rho_\infty u_\infty} \qquad (2.3.2)$$

where we have used (2.2.13) to obtain the representation in terms of lift. Now define the total vorticity in the half plane by

$$\Gamma_0 = \int_{T_{1/2}} \omega_x dS \tag{2.3.3}$$

and the lateral separation (distance between centers) of axial vorticity by

$$\bar{y} = \frac{1}{\Gamma_0} \int_T y\omega_x dS \tag{2.3.4}$$

Then (2.3.2) may be written as

$$L = \rho_\infty u_\infty \Gamma_0 \cdot \bar{y} \tag{2.3.5}$$

the famous Kutta Joukowsky formula for lift. Also

$$\int_T z\omega_x = \int_T v dS = 0 \tag{2.3.6}$$

since we have postulated a plane of symmetry with no net side force.

Now consider transverse moments of ω_y and ω_z. We get

$$\int_T dS\ z\cdot\omega_y = \int_T (u_\infty - u) dS - \frac{d}{dx} \int_T zw dS$$

$$\int_T dS\ y\omega_z = - \int_T (u_\infty - u) dS + \frac{d}{dx} \int_T yw dS \tag{2.3.7}$$

The last term in each of the above expressions is assumed to be zero. All vorticity moments that exist must be adiabatic invariants (with respect to x)

in the intermediate wake region where Trefftz plane arguments are valid. Thus we have an expression for the momentum loss associated with the axial flow that is the first major component of the drag (see (2.2.10) and (2.2.11)). We write

$$\int_T (P_\infty - P)dS = \int_T \rho_\infty u_\infty (u_\infty - u)dS$$

$$= \rho_\infty u_\infty \int_T dS\ z \cdot \omega_y$$

$$= -\rho_\infty u_\infty \int_T dS\ y \cdot \omega_z$$

$$= \frac{\rho_\infty u_\infty}{2} \int_T dS(z\omega_y - y\omega_z) \qquad (2.3.8)$$

For the moment we refrain from giving this drag component a name.

The second moments of axial vorticity are related to the angular momentum and root bending moment. We calculate

$$\int_{T_{1/2}} (y^2+z^2)\omega_x\ dS = -2 \int_{T_{1/2}} (yw-zv)dS - \int_{\substack{-\infty \\ y=0}}^{\infty} z^2 w dz \qquad (2.3.9)$$

and note that the first term is proportional to the flux of angular momentum through the half Trefftz plane. But from (2.2.14), we have for the root bending moment

$$M = \rho_\infty u_\infty \int_{T_{1/2}} (yw-zv)dS + \int_{y=0} (p-p_\infty) \cdot z\ dxdz \qquad (2.3.10)$$

Combining the last two equations, we get

$$M = -\frac{\rho_\infty u_\infty}{2}\int_{T_{1/2}} (y^2+z^2)\omega_x dS - \frac{\rho_\infty u_\infty}{2}\int_{\substack{-\infty \\ y=0}}^{\infty} z^2 w\, dz$$

$$+ \int_{y=0} (p-p_\infty)\cdot z\, dxdz \qquad (2.3.11)$$

For high aspect ratio configurations, the integrals over $y = 0$ in (2.3.11) can be omitted. The root bending moment is the flux of angular momentum and also the polar moment of the wake axial vorticity distribution; i.e.;

$$M \cong \rho_\infty u_\infty \int_{T_{1/2}} (yw-zv)dS$$

$$= -\frac{\rho_\infty u_\infty}{2}\int_{T_{1/2}} (y^2+z^2)\omega_x dS \qquad (2.3.12)$$

The last result is a fundamental building block in the Betz theory of wake roll up (Ref. 8).

The final moment of vorticity that we consider is nonlinear. Introduce the vector stream function $\vec{\psi}$ such that

$$\vec{v} = \text{curl}\ \vec{\psi} \quad \text{with} \quad \text{div}\ \vec{\psi} = 0 \qquad (2.3.13)$$

Then we get

$$\omega_x = -\left(\frac{\partial^2\psi_x}{\partial y^2} + \frac{\partial^2\psi_x}{\partial z^2}\right) - \frac{\partial^2\psi_x}{\partial x^2} \qquad (2.3.14)$$

Based on the notion of adiabatic invariance of wake properties we neglect the last term in (2.3.14) and write

$$\frac{\partial^2 \psi_x}{\partial y^2} + \frac{\partial^2 \psi_x}{\partial z^2} = - \omega_x \tag{2.3.15}$$

Also, to the same order of approximation the velocity components in the Trefftz plane are given by

$$v = \frac{\partial \psi_x}{\partial z} \quad , \quad w = - \frac{\partial \psi_x}{\partial y} \tag{2.3.16}$$

Now compute

$$\int_T \omega_x \psi_x dx = - \int_T \psi_x \left(\frac{\partial^2 \psi_x}{\partial y^2} + \frac{\partial^2 \psi_x}{\partial z^2} \right) dS$$

$$= \int_T (v^2+w^2) dS \tag{2.3.17}$$

with an integration by parts. But we can also solve (2.3.15) in the Trefftz plane to get

$$\psi_x = - \frac{1}{2\pi} \int_T \omega_x \, \ell n \, |\vec{x}-\vec{y}| \, d^2\vec{y} \tag{2.3.18}$$

Now combine (2.3.17) and (2.3.18) and use (2.2.12) to obtain the following expression for that component of drag that is proportional to kinetic energy of the cross flow in the Trefftz plane:

$$\int_T (p_\infty - p) dS = \int_T \frac{\rho v_1^2}{2} dS$$

$$= - \frac{\rho_\infty}{4\pi} \int_T \omega_x(\vec{x}) d^2\vec{x} \int_T \omega_x(\vec{y}) d^2\vec{y} \, \ell n |\vec{x}-\vec{y}| \tag{2.3.19}$$

Thus, the lift, root bending moment and the above component of drag depend only on the streamwise component of vorticity. The first two are linearly dependent on ω_x while the drag is quadratically dependent on ω_x. For convenience we summarize the key formula of this section below:

Summary

$$L = \rho_\infty u_\infty \Gamma_0 \cdot \bar{y} \qquad \Gamma_0 = \int_{T_{1/2}} \omega_x dS \qquad \bar{y} = \frac{1}{\Gamma_0} \int_T y\omega_x dS$$

$$M \cong -\frac{\rho_\infty u_\infty}{2} \int_{T_{1/2}} (y^2+z^2)\omega_x dS$$

$$\int_T (p_\infty - p) dS = \int_T \frac{\rho v^2}{2} dS$$

$$= -\frac{\rho_\infty}{4\pi} \int_T \omega_x(\vec{x}) d^2\vec{x} \int_T \omega_x(\vec{y}) d^2\vec{y} \; \ell n|\vec{x}-\vec{y}|$$

$$\int_T (P_\infty - P) dS = \rho_\infty u_\infty \int_T (u_\infty - u) dS$$

$$= \frac{\rho_\infty u_\infty}{2} \int_T (z\omega_y - y\omega_z) dS \qquad (2.3.20)$$

The total drag is the sum of the last two relations in (2.3.20) and is expressed entirely in terms of integral properties of the vorticity in the Trefftz plane; i.e.,

$$D = \frac{\rho_\infty u_\infty}{2} \int_T (z\omega_y - y\omega_z) dS - \frac{\rho_\infty}{4\pi} \cdot \int_T \omega_x d^2\vec{x} \cdot \int_T \omega_x d^2\vec{y} \; \ell n|\vec{x}-\vec{y}| \qquad (2.3.21)$$

To conclude this section we present formula for the drag in terms of properties of a typical rolled up vortex wake. Within a few spans downstream of a lifting wing the axial and azimuthal vorticity assume a more or less radial distribution about two well defined centers that are separated by the parameter $\bar{y}$ given in (2.3.20). The situation is illustrated in Figure 2. The integrals in (2.3.21) can be expressed in terms of $\omega_\theta(r)$ (the aximuthal vorticity associated with the axial momentum defect) and $\omega_x(r)$, the axial or streamwise vorticity. We note that

$$y = \bar{y} + r\cos\theta \qquad z = r\sin\theta$$

$$\omega_y = \omega_\theta \sin\theta \qquad \omega_z = -\omega_\theta \cos\theta \tag{2.3.22}$$

Thus

$$\int_T (P_\infty - P)dS = \frac{\rho_\infty u_\infty}{2}\int_T (z\omega_y - y\omega_z)dS$$

$$= \rho_\infty u_\infty \int_0^\infty r dr \int_0^{2\pi} d\theta\left[r\omega_\theta \sin^2\theta + (\bar{y}+r\cos\theta)\, r\cos\theta\right]$$

$$= \rho_\infty u_\infty \cdot 2\pi \int_0^\infty \omega_\theta\, r^2 dr \tag{2.3.23}$$

Introduce the following definitions of total azimuthal vorticity Γ_θ and the radial spread r_θ:

$$\Gamma_\theta = 2\pi \int_0^\infty r\omega_\theta dr$$

$$r_\theta = \frac{2\pi}{\Gamma_\theta}\int_0^\infty r^2\omega_\theta dr \tag{2.3.24}$$

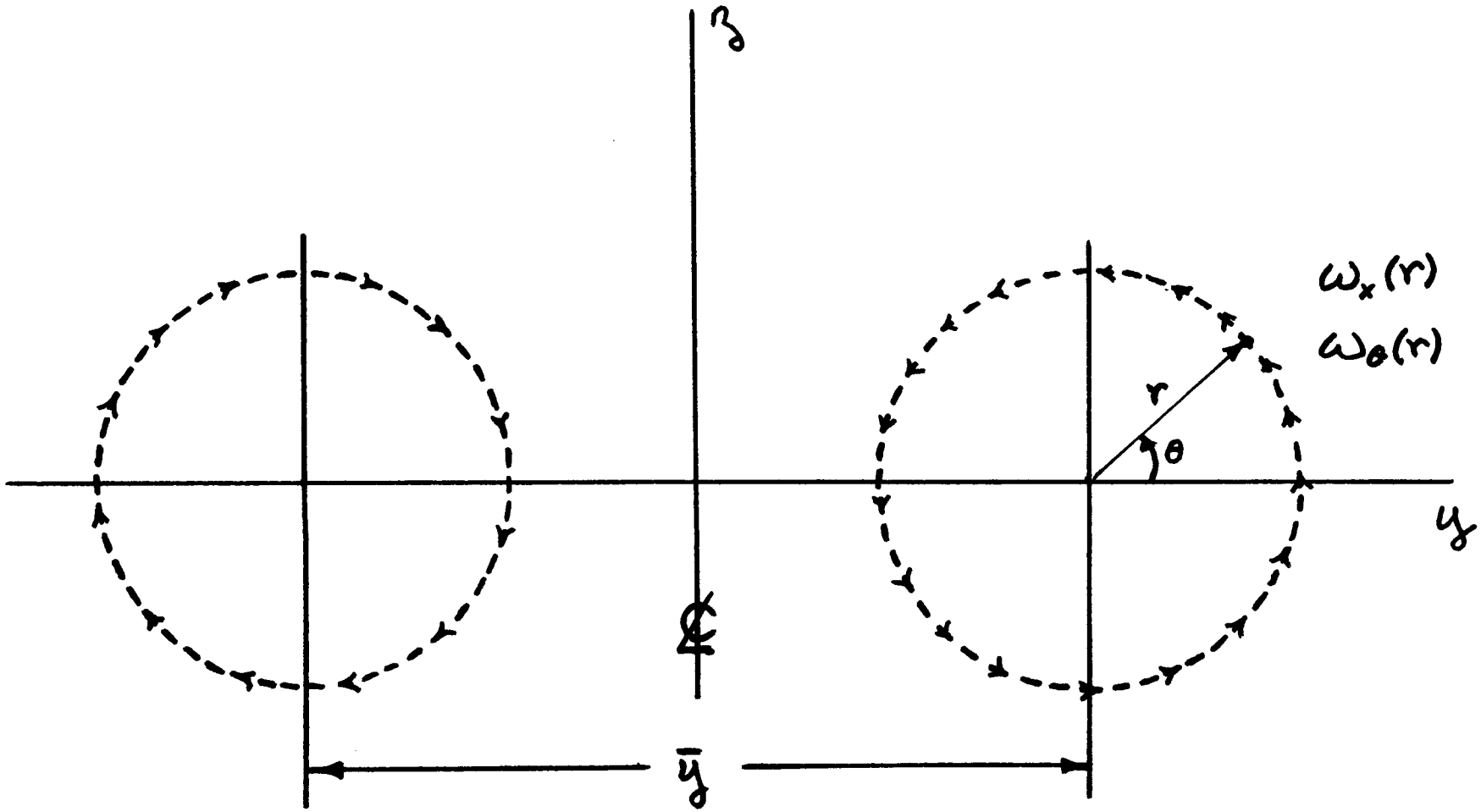

Figure 2.2 - Trefftz Plane Representation of Wake Vorticity of a Lifting Wing.

Thus, we obtain for (2.3.23)

$$\int_T (P_\infty - P)dS = \rho_\infty u_\infty \Gamma_\theta \cdot r_\theta \qquad (2.3.25)$$

Thus the drag associated with the total head loss can be expressed in the rolled-up region of the Trefftz plane by a formula that is directly analogous to the Kutta Joukowski formula for lift.

The second term in the expression for drag (2.3.21) can also be expressed in terms of the total circulation associated with lift and an integral length scale that is a measure of the spread of the axial vorticity. We get

$$\int_T \frac{\rho v^2}{2}\, dS = \frac{\rho \Gamma_0^2}{2\pi} \ell n\, \bar{y}/\ell_o$$

$$= \frac{1}{2\pi\rho u_\infty^2} \frac{L^2}{\bar{y}^2} \ell n\, \bar{y}/\ell_o \qquad (2.3.26)$$

where the integral scale, ℓ_o, is given by the solution of the following equation:

$$\int_0^{\ell_o} \frac{\Gamma}{\Gamma_0} \frac{dr}{r} - \int_{\ell_o}^{\infty} \left(1 - \frac{\Gamma}{\Gamma_0}\right)\frac{dr}{r} = \int_0^{\infty} \frac{\Gamma}{\Gamma_0}\left(1 - \frac{\Gamma}{\Gamma_0}\right)\frac{dr}{r} \qquad (2.3.27)$$

where $\Gamma(r)$ is the circulation distribution in the rolled up vortex. If the drag associated with the cross flow kinetic energy is reduced to a drag coefficient, C_{D_i}, based on the total area S. Then

$$C_{D_i} = \frac{1}{q_\infty \cdot S} \int_T \frac{\rho v^2}{2}\, dS$$

$$= \frac{C_L^2}{\pi A}\left[\left(\frac{b}{\bar{y}}\right)^2 \ell n \left(\frac{\bar{y}}{\ell_o}\right)^{1/4}\right] \qquad (2.3.28)$$

For a wing that is elliptically loaded, it is well known that the expression in brackets is exactly unity with

$$\frac{\bar{y}}{b} = \frac{\pi}{4} \quad , \quad \frac{\ell_o}{\bar{y}} = e^{-\pi^2/4} \tag{2.3.29}$$

Thus we have derived an expression for the "induced drag" including a formula for the efficiency factor. That is, if

$$C_{D_i} = \frac{C_L^2}{\pi A e} \tag{2.3.30}$$

then

$$e = \left(\frac{\bar{y}}{b}\right)^2 \cdot \frac{1}{\ell n(\bar{y}/\ell_o)^{1/4}} \tag{2.3.31}$$

We will give estimates of the induced drag based on the above formula. This is the first major component of drag-due-to-lift. It is not the whole story, however. The drag associated with the total head loss is also dependent on the lift as we will demonstrate below.

2.4 Drag and Lift in Terms of Surface Pressure

In the last two section we have concentrated on representations of drag and lift in the Trefftz plane. It is informative to supplement the above results with near field surface representations of drag and lift. We concentrate on the contribution of the pressure to lift and drag of a wing. From (2.1.7) and (2.1.8) we have

$$L = -\int_S p\vec{k}\cdot\vec{n}\, dS \tag{2.4.1}$$

$$D = -\int_S p\vec{i}\cdot\vec{n}\, dS \qquad \text{(Pressure drag)} \tag{2.4.2}$$

Now suppose that the wing has upper and lower surfaces defined by

$$S: z^{\pm} = \pm \underset{\text{Thickness}}{\varepsilon f(x,y)} + \underset{\substack{\text{Camber} \\ \& \text{ Twist}}}{\delta g(x,y)} - \underset{\text{Angle of attack}}{\alpha x} \tag{2.4.3}$$

Also, we define mean and difference pressure coefficients and lift and drag coefficients as follows:

$$\sigma = \frac{1}{2}(p^+ + p^-)/q_\infty = \frac{C_p^+ + C_p^-}{2} \quad \text{Mean Pressure Coefficient} \tag{2.4.4}$$

$$\Delta = (p^- - p^+)/q_\infty = C_p^- - C_p^+ \quad \text{Difference Pressure Coefficient} \tag{2.4.5}$$

$$C_L = \frac{L}{q_\infty \cdot S} \tag{2.4.6}$$

$$C_D = \frac{D}{q_\infty \cdot S} \tag{2.4.7}$$

Now assume that Δ and σ are regular functions of α and δ and expand C_L to first order and C_D to second order in α and δ. The results are:

$$C_D(\alpha,\delta) = C_{D_0} + \left(C_{L_\alpha} + \varepsilon \iint_S \left(\frac{\partial^2 \sigma}{\partial \alpha^2}\right)_0 f_x \frac{dxdy}{S} \right) \alpha^2$$

$$+ \left(C_{L_\delta} - \iint_S \left(\frac{\partial \Delta}{\partial \alpha}\right)_0 g_x \frac{dxdy}{S} + 2\varepsilon \iint_S \left(\frac{\partial^2 \sigma}{\partial \alpha \partial \delta}\right)_0 f_x \frac{dxdy}{S} \right) \alpha \cdot \delta$$

$$+ \left(\varepsilon \iint_S \left(\frac{\partial^2 \sigma}{\partial \delta^2}\right)_0 f_x \frac{dxdy}{S} - \iint_S \left(\frac{\partial \Delta}{\partial \delta}\right)_0 g_x \frac{dxdy}{S} \right) \delta^2 \tag{2.4.8}$$

$$C_L(\alpha,\delta) = C_{L_\alpha}\cdot\alpha + C_{L_\delta}\cdot\delta \tag{2.4.9}$$

with

$$C_{D_0} = 2\varepsilon \iint_S (\sigma)_0 \, f_x \, \frac{dxdy}{S} \tag{2.4.10}$$

$$C_{L_\alpha} = \iint_S \left(\frac{\partial \Delta}{\partial \alpha}\right)_0 \frac{dxdy}{S} \tag{2.4.11}$$

$$C_{L_\delta} = \iint_S \left(\frac{\partial \Delta}{\partial \delta}\right)_0 \frac{dxdy}{S} \tag{2.4.12}$$

Many interesting results can be derived with (2.4.8) and its counterpart that accounts for the drag due to the surface viscous stress. Here we want to show the connection between drag and lift due to pressure for the simple case of a wing with symmetric airfoil sections (zero camber). With $\delta = 0$, we get

$$C_D(\alpha) = C_{D_0} + \left(C_{L_\alpha} + \varepsilon \iint_S \left(\frac{\partial^2 \sigma}{\partial \alpha^2}\right)_0 f_x \cdot \frac{dxdy}{S}\right)\alpha^2 \tag{2.4.13}$$

$$C_L(\alpha) = C_{L_\alpha}\cdot\alpha \tag{2.4.14}$$

or

$$C_D(\alpha) = C_{D_0} + K\cdot C_L^2 \tag{2.4.15}$$

with

$$K = \frac{1}{C_{L_\alpha}} + \frac{\varepsilon}{C_{L_\alpha}^2} \iint_S \left(\frac{\partial^2 \sigma}{\partial \alpha^2}\right)_0 f_x \cdot \frac{dxdy}{S} \tag{2.4.16}$$

The second term in (2.4.15) is of the same form as the induced drag formula (2.3.29) and in fact if we were clever enough to derive the pressure distribution on the three dimensional wing to second order in α we could in fact calculate the induced drag with (2.4.16). That would be a very difficult task and is not necessary. The point of (2.4.16) is to illustrate sources of drag-due-to-lift that are not contained in (2.3.29). The familiar "induced" component of drag-due-to-lift is actually the drag due to the spanwise variation of lift. It is the price we pay for flying a wing of finite span. However even if the span is infinite and the load is uniform the drag of a symmetric airfoil section varies quadratically with angle of attack and therefore with the lift. The formula (2.4.15) can then be replaced with section properties; i.e.,

$$c_d(\alpha) = c_{d_0} + kc_\ell^2$$

with

$$k = \frac{1}{c_{\ell_\alpha}} + \frac{\varepsilon}{c \cdot c_{\ell_\alpha}^2} \int_0^c \left(\frac{\partial^2 \alpha}{\partial \alpha^2} \right)_0 f_x \cdot dx \qquad (2.4.17)$$

The section profile drag-due-to-lift is characterized by the parameter

$$k = \frac{dc_d}{dc_\ell^2} \qquad (2.4.18)$$

The second term in (2.4.17) (also in (2.4.13)) shows the effect of thickness on drag-due-to-lift. If ε tends to zero and the integral remains bounded then

$$\lim_{\varepsilon \to 0} k = \frac{1}{c_{\ell_\alpha}} = \frac{1}{2\pi} \cong 0.16 \quad \text{Flat Plate Airfoil Section} \qquad (2.4.19)$$

where 2π is the standard lift coefficient for a flat plate airfoil. On the other hand, for a wide class of airfoil sections, k is at least an order of magnitude smaller than $1/2\pi$. In Table 1 we have calculated k for airfoil section data from Abbott & VanDoenhoff (Ref. 9). The data are for sections with standard leading edge roughness. In general k is about the same order of magnitude as the profile drag coefficient; i.e., $c_{d_0} \cong 0.01$. For the thinner sections k is somewhat greater than c_{d_0}. However, Hoerner (Ref. 10)

Table 1. Section Drag Due to Lift ($R_e \tilde{=} 10^6$).

Airfoil Section NACA	$\frac{dc_d}{dc_\ell^2}$	Airfoil Section NACA	$\frac{dc_d}{dc_\ell^2}$
006	.013	64015	.01
009	.012	64018	.01
012	.013	64021	.019
63012	.011	64A010	.014
63015	.0094		
63018	.0094	65006	.014
63A010	.0125	65015	.01
		65018	.012
64006	.034	65021	.011
64009	.0147		
64012	.012	Flat Plate	$1/2\pi \simeq .159$

recommends that the parameter k be replaced by c_{d_o} in calculating section drag due to lift. Also we note the experimental data in Ref. 10 (7-3, Fig. 4) that shows the abrupt increase in k for the flat plate section. Clearly the pressure force on a flat plate must be normal to the plate and that means a drag for small α of the form

$$c_{d_i} = c_\ell \cdot \alpha$$

But

$$\alpha = c_\ell / c_{\ell_\alpha} = c_\ell / 2\pi$$

so that

$$c_{d_i} = \frac{c_\ell^2}{2\pi} \quad \text{or} \quad k = 1/2\pi \tag{2.4.20}$$

the same as (2.4.19).

It is well known, of course, that the large flat plate section drag is due to the absence of leading edge suction. On the other hand if the parameter k in (2.4.17) is calculated with exact two-dimensional airfoil theory, the result is zero, even in the limit as $\varepsilon \to 0$ (the d'Alembert paradox). The small experimental values for k in Table 1 indicate that reasonably good potential flow is established over airfoil sections. The above observations suggest a method for calculating the pressure contribution to the section drag-due-to-lift. We write

$$\sigma = \sigma_p + \Delta\sigma \tag{2.4.21}$$

where σ_p is the mean pressure coefficient calculated with potential theory and $\Delta\sigma$ is the difference between the true value and σ_p. Substitute (2.4.21) into (2.4.17) and note that the potential part of the integral cancels the leading term c_{ℓ_α}. Thus, we get

$$k = \frac{\varepsilon}{c \cdot c_{\ell_\alpha}^2} \int_0^c \left(\frac{\partial^2 \Delta\sigma}{\partial \alpha^2} \right)_0 f_x \cdot dx \tag{2.4.22}$$

The above formula is useful if the airfoil section has been properly designed

to avoid leading edge separation. Then the main contribution to section drag-due-to-lift is the lack of pressure recovery over the aft part of the airfoil and that in turn is due to the viscous boundary layer (Recall that all drag and lift is due to viscosity).

In addition to the pressure contribution there is also a direct viscous contribution to the section drag (see (2.1.8)). Following, Hoerner (Ref. 10, 6-11) we note that from the Kutta Joukowski formula for lift that there is an average circulation velocity around an airfoil section; i.e.,

$$\Gamma = \oint_{\text{airfoil}} w \, ds \cong w_{av} \cdot 2c = \frac{c_\ell \cdot u_\infty \cdot c}{2} \tag{2.4.23}$$

so that

$$\frac{w_{av}}{u_\infty} = \frac{c_\ell}{4} \qquad \text{Circulation velocity} \tag{2.4.24}$$

This circulation velocity adds to the velocity near the upper surface and subtracts on the lower surface. Thus the skin friction drag can be written as

$$c_d \cong c_f \cdot \left(\frac{q^+}{q_\infty} + \frac{q^-}{q_\infty} \right)$$

$$= c_f \left(\left(1 + \frac{w_{av}}{u_\infty} \right)^2 + \left(1 - \frac{w_{av}}{u_\infty} \right)^2 \right)^2$$

$$= 2 \, c_f \left(1 + \left(\frac{w_{av}}{u_\infty} \right)^2 \right)$$

$$= 2 \, c_f + \frac{c_f}{8} \cdot c_\ell^2 \tag{2.4.25}$$

where c_f is the flat plate skin friction drag coefficient. Thus the direct viscous contribution to section drag-due-to-lift is

$$k_v = \frac{c_f}{8} \tag{2.4.26}$$

which result we may add to (2.4.20) to get

$$k = \underbrace{\frac{c_f}{8}}_{\text{Viscosity}} + \frac{\varepsilon}{c_{\ell_\alpha}^2} \int_0^c \underbrace{\left(\frac{\partial^2 \Delta\sigma}{\partial \alpha^2}\right)_0}_{\text{Pressure}} \cdot f_x \cdot \frac{dx}{c} \tag{2.4.27}$$

For Reynolds numbers of order 10^6 or 10^7 the turbulent flat plate skin friction coefficient is of order .002 to .003, so that the viscous contribution to k is of order .00025 to .0004. Thus we conclude from the experimental data (Table 1) that the main source of section drag-due-to-lift is the lack of pressure recovery over the section trailing edge or absence of leading edge suction. Both sources are a result of deviation of the surface pressure from the ideal potential flow value. The above conclusion is valid for turbulent airfoil sections. If laminar flow can be maintained on the section and the boundary layer kept thin, then values of k considerably smaller than 0.01 can be realized. This is a viable approach to reducing the section drag-due-to-lift. Also we point out that we have completely ignored the contribution of section camber in the foregoing discussion. With a properly cambered section the effective k in our section drag formula can be reduced to zero for c_ℓ measured from the optimum lift. The analytic results needed to achieve the optimum can be deduced from (2.4.8) - a worthwhile task.

2.5 A Practical Wing - Drag Formula

We are now in a position to write a single expression for wing drag with a useful decomposition of the drag-due-to-lift. For drag we write

$$D = \int_{\text{Span}} c_d(y) \cdot q_\infty \cdot c(y) \cdot dy + D_i$$

or

$$C_D = \frac{1}{S} \int_{\text{Span}} c_d(y) \cdot c(y) \cdot dy + C_{D_i} \tag{2.5.1}$$

where C_{D_i} is the induced drag due to finite span (Section 2.3) and the integral must account for the section drag that is independent of aspect

ratio. With the section drag results obtained in Section 2.4 we get

$$C_D = C_{D_0} + \frac{1}{S}\int_{\text{Span}} k(y)\cdot c(y)\cdot c_\ell^2\, dy + C_{D_i} \tag{2.5.2}$$

on

$$C_D = C_{D_0} + \left(\lambda_s + \frac{1}{\pi Ae}\right) C_L^2 \tag{2.5.3}$$

where C_{D_0} is the wing profile drag (at zero lift) and

$$\lambda_s = \frac{S\int_{\text{Span}} k(y)\cdot c_\ell^2\cdot c(y)dy}{\left(\int_{\text{Span}} c_\ell(y)\cdot c(y)dy\right)^2}$$

$$\cong \frac{1}{S}\int_{\text{Span}} k(y)\cdot c(y)dy \tag{2.5.4}$$

where we have used the typical section lift coefficient $c_\ell = 2\pi\alpha$. We further decompose (2.5.4) with our knowledge of k(y) obtained in the last section. For most of the wing span k(y) can be replaced with the average section drag coefficient. However, if a fraction of the leading edge (say ℓ_s/b) is separated then k is about $1/2\pi$ for those sections. Thus, we can write

$$\lambda_s = c^*_{d_s} + \frac{1}{2\pi}\left(\frac{\ell_s}{b}\right)$$

and for the wing drag

$$C_D \cong C_{D_0} + \left[\underbrace{c^*_{d_s} + \frac{1}{2\pi}\left(\frac{\ell_s}{b}\right)}_{\text{Section DDL}} + \underbrace{\frac{1}{\pi Ae}}_{\text{Induced DDL}}\right] C_L^2 \tag{2.5.5}$$

with

$c^*_{d_s}$ = average section profile drag coefficient

ℓ_s/b = fraction of span that has a separated leading edge flow

A = aspect ratio

$$e = \left(\frac{\bar{y}}{b}\right)^2 / \ell n(\bar{y}/\ell_o)^{1/4} \quad \text{(see (2.3.30))} \tag{2.5.6}$$

The last formula is the basis for our evaluation in Section 3 of various devices and techniques that have been proposed to reduce the drag-due-to-lift.

Before moving into the realm of drag estimation we call attention to the close relationship between our basic drag formula (2.5.5) and the more formal result (2.3.21) that expresses the drag in terms of Trefftz plane moments of vorticity . Recall that the induced drag formula was derived quite rigorously from the logarithmic correlation of axial shed vorticity in (2.3.21). Our results for section drag were obtained with more heuristic arguments that were based on the surface pressure representation of drag and a mixture of experimental results. Actually, the first term in (2.3.21) is a direct representation of the section drag in the Trefftz plan. To see this we recall(see (2.3.8)) that the first term can be expressed in the form

$$D_s = \rho_\infty u_\infty \int_T z\omega_y dS$$

or

$$C_{D_s} = \frac{2}{u_\infty S}\int_T z\omega_y dS \tag{2.5.7}$$

$$\cong \frac{2}{u_\infty S}\int_{\text{Span}} dy \int_{-\infty}^{\infty} dz \cdot z \frac{\partial}{\partial z}(u-u_\infty)$$

$$\cong \frac{2}{S}\int_{\text{Span}} \delta_w^*(y)dz \qquad (2.5.8)$$

where

$$\delta_w^*(y) = \int_{-\infty}^{\infty}\left(1 - \frac{u}{u_\infty}\right)dz \qquad (2.5.9)$$

is the wake displacement thickness in a Trefttz plane sufficiently far downstream that the difference between the wake momentum and displacement thickness is small (i.e., several chords). We can further write for a symmetric airfoil section

$$\delta^* = \delta_o^* + \frac{1}{2}\left(\frac{\partial^2\delta^*}{\partial\alpha^2}\right)_0 \cdot\alpha^2 + \text{Higher Order Terms}$$

so that

$$C_{D_s} = \frac{2}{S}\int_{\text{Span}} \delta_o^* dy + \frac{1}{S}\int_{\text{Span}} \left(\frac{\partial^2\delta^*}{\partial\alpha^2}\right)_0 dy \cdot \frac{C_L^2}{C_{L_\alpha}^2} \qquad (2.5.10)$$

From the last relation we note that the section drag-due-to-lift is the direct result of the second order increase of wake displacement (or momentum) thickness with angle of attack. Clearly the wake thickness will increase abruptly if the leading edge separates. Also, the wake thickness will increase because of the enhanced adverse pressure gradient over the aft section of the airfoil. Both of these effects are contained in the basic drag formula (2.5.5). Also, it is worth noting that the section drag-due-to-lift is primarily associated with the spanwise component of vorticity and hence with the chordwise variation of the load. The familiar induced drag is associated with the shed streamwise vorticity that is a direct result of spanwise load variations. The expression "drag-due-to-lift" is in fact a misnomer. A more descriptive term would be "drag due to load variation".

3. AN ASSESSMENT OF CONVENTIONAL DRAG-DUE-TO-LIFT REDUCTION DEVICES AND TECHNIQUES

The purpose of this section is to quantitatively assess the relative merits of various ideas that have been proposed to reduce drag-due-to-lift. The objective is to draw attention to those areas where the biggest payoffs might be. We focus initially on methods for CTOL wings and progress to out of plane configurations in subsequent sections.

3.1 Planform Shape (Load variation on a Plane)

The CTOL wing planform is the most extensively studied (both experimentally and theoretically) lifting configuration that has evolved in the aeronautics industry. Because of its long history of engineering development it has been "optimized" for all practical purposes. In fact we can most easily illustrate the idea of an optimum configuration with the CTOL wing.

It is well known that the induced drag of the CTOL wing is a minimum when the load is elliptic. The induced drag coefficient is

$$C_{D_i} = \frac{C_L^2}{\pi A} \tag{3.1.1}$$

This famous result is usually derived with lifting line theory - a linear high aspect ratio approximation. Because of the approximations of the linear theory one might question the validity of the induced drag result. However, when the drag of "well designed" wings is compared to this result the differences are of the order of a percent or so (e.g., see Figures 4 and 10, Section 7-6 of Hoerner (Ref. 10). Even the drag of the delta wing and other small aspect ratio configurations correlates reasonably well with the theoretical minimum (e.g., see Figure 28, Section 7-17, Hoerner), as long as the leading edge is profiled. The reason is that the theoretical result is much more general than classical lifting line theory would indicate. In fact it follows from the general drag formulas developed herein. For example with (2.2.10) and (2.3.14) we note that if all near field total head loses are neglected then the drag minimum can be expressed as

$$D \geq \int_T \frac{\rho v_i^2}{2}\, dS \qquad \text{Minimum Drag}$$

$$= -\frac{\rho_\infty}{4\pi} \int_T \omega_x d^2\vec{x} \int_T \omega_x d^2\vec{y}\ \ell n|\vec{x}-\vec{y}| \tag{3.1.2}$$

independent of any other statements about lifting line theory. The lift also is given quite generally by the formula

$$L = \rho_\infty u_\infty \int_T y\omega_x dS \qquad (3.1.3)$$

The minimization of (3.1.2) in the Trefftz plane subject to the constraint of a given airplane lift leads directly to the famous induced drag formula (3.1.1) for the CTOL wing or any other wing (even of small aspect ratio) whose projection on the Trefftz plane is a straight line.

It is absolutely essential in any discussion of drag-due-to-lift to be aware of the theoretical minimum that could be achieved if all near field total head losses could be eliminated. The drag-due-to-lift of the perfect CTOL airplane would be the same as the ideal wing induced drag (3.1.1). Over the years of CTOL airplane development the ideal induced drag fraction of drag-due-to-lift has increased as parasitic and interference sources of drag-due-to-lift have decreased. For example, the induced drag fraction of the Me-109 was only 69% (Hoerner, p. 14-12). The total drag-due-to-lift at optimum cruise is one half of the total drag, a direct result of the airplane drag polar. There is still room for improvement in reducing parasitic and interference sources of drag-due-to-lift. Innovative ideas for mating lifting and non-lifting airplane components should be explored in current CTOL drag research programs. However, the CTOL wing alone is a highly efficient drag device, within a few percent of the theoretical minimum drag-due-to-lift if good design practice is followed. The wing tip is an important element of the overall wing design. However, the technology is available (Ref. 11) for designing a CTOL wing tip with less than 0.5% of airplane drag (e.g., the Boeing 757). The main point is that efforts to refine the CTOL wing induced drag efficiencies are reaching a point of diminishing returns. Improvements of the order of a fraction of a percent are about the best one can hope for. If these improvements can be discovered, tested and implemented easily at the airplane operational level, then they might be economical. A complete wing redesign to achieve a half a percent drag reduction would be hard to justify.

Because the well designed CTOL wing is nearly optimal, we can argue that small modifications to the trailing edge will have little or no effect on the drag-due-to-lift. It has been known for many years (Hoerner, p3-22, Fig. 4.2) that an airfoil section with a slightly blunted trailing edge (= 0.4% thickness) has a lower drag at finite lift then the same section with a sharp trailing edge although the form drag is usually greater. With a sharp trailing edge the upper surface separation line migrates forward with increasing angle of attack starting at a very small value of lift; hence, the nearly parabolic increase of section drag-due-to-lift. With a cut off trailing edge the separation point is held at the cutoff edge to a much higher angle of attack. The section drag rise with lift does not occur until some lift coefficient above the design lift coefficient and hence the lower

drag-due-to-lift. In terms of our drag formula (2.5.5)

$$C_D = C_{D_0} + \left[c^*_{d_s} + \frac{1}{2\pi}\left(\frac{\ell s}{b}\right) + \frac{1}{\pi A e}\right] C_L^2 \qquad (3.1.4)$$

this means that the term $c^*_{d_s}$ is virtually zero and the overall wing drag-due-to-lift is brought even closer to the theoretical optimum value. These remarks apply equally to the use of serrated trailing edges. There is in our opinion no fundamental mechanism for edge serrations to affect the overall load distribution and the theoretical drag minimum. However, they can perhaps be used effectively to maintain attached flow over the aft portion of each wing section, reduce $c^*_{d_s}$, and more closely achieve the optimum drag.

3.2 Out of Plane Tip Devices

We have discussed the CTOL wing as an example of a lifting configuration that has been optimized for all practical purposes. The engineering techniques required to achieve an optimal design have evolved over a period of many years and for the most part are understood. If there is to be a significant reduction (10% say) of wing drag-due-to-lift then it must come from new wing concepts based on a deeper understanding of underlying principles. Several concepts have surfaced over the past decade and deserve to be considered seriously. The winglet, tip-feathers, and sails (Refs. 2,3,4 & 5) fall in the category of out-of-plane devices and must be assessed in their own right. For each configuration there is a theoretical minimum induced drag (a Carnot efficiency if you will). Each new design must be evaluated by comparing the experimentally achieved drag to the theoretical minimum. If the theoretical minimum drag for a selected configuration is less than the minimum for a CTOL wing then there is an excellent chance of designing a more efficient cruise wing. If the theoretical minimum is greater then you will never do better than the CTOL wing although other factors may dictate the new design. In this regard we are well aware that induced drag efficiency is not the only number that dictates a wing design. However, in the following we will discuss out-of-plane wing concepts primarily from the point of view of reducing the theoretical minimum induced drag.

The basic principle of all out-of-plane devices is contained in the simple formula (2.5.6) for the ideal wing efficiency; i.e.;

$$e = \left(\frac{\bar{y}}{b}\right)^2 / \ell n \left(\frac{\bar{y}}{\ell_o}\right)^{1/4} \qquad (3.2.1)$$

where b is the wing span, $\bar{y}$ is the spanwise distance between the shed lifting vortex centers (vortex span) and ℓ_o is the integral spread scale of the rolled up vorticity. For the optimally loaded (elliptic) CTOL wing we have

$$\frac{\bar{y}}{b} = \frac{\pi}{4} \quad , \quad \frac{\ell_o}{b} = \frac{\pi}{4} e^{-\pi^2/4} \cong .067, \quad e = 1.0 \qquad (3.2.2)$$

The integral spread scale is 6.7% of the span or about a mean aerodynamic chord for an aspect ratio of 6 or 7. Roughly speaking, ℓ_o scales with the difference between the wing span and vortex span (i.e., $b-\bar{y}$). If the CTOL wing tip is overloaded (rectangular, e.g.) the advantage of making $\bar{y}$ bigger (it cannot exceed b) is offset by the diminished spread scale and the induced drag becomes greater. However, if the lift induced tip vorticity can be diffused vertically, the integral scale can in principal be controlled independently of $\bar{y}$ as the tip is loaded. This is one way of explaining how winglets, tip feathers, etc. can lead to a smaller value of wake kinetic energy and induced drag for the same circulation. It is the same principle that explains the bi-wing or multi-wing. How much drag reduction can be achieved? A calculation with minimum induced drag theory (e.g., Ref. 12,13 & 14) must be carried out to obtain a precise number. However, an estimate of potential drag reduction can be made with (3.2.1).

In Figure 3.1 we have plotted the normalized integral spread scale ℓ_o/b versus the vortex span $\bar{y}/b$ for constant values of the efficiency e. Point A on the curve for e=1 is the conventional CTOL wing that is elliptically loaded (3.2.2). For a given configuration the load distribution will determine a unique point in Figure 3.1 and if the load distribution has been optimized the largest value of e will be attained. As an example suppose that with a suitable wing tip device the vortex span $\bar{y}/b$ is increased from $\pi/4$ to 0.89. If the tip device maintains the same vortex integral scale as the CTOL wing ($\ell_o/b \cong 0.067$) then the efficiency can be increased by about 20% (e = 1.2 or point B in Figure 3.1). To achieve this result the tip device would have to have a vertical dimension of the order .067b and be optimally loaded. With a tip device of only .037b the unit efficiency of the CTOL wing can be maintained (point C in Figure 3.1). In general, if the wing can be loaded at the tip so that $\bar{y}/b$ is increased, the size of a tip device to achieve a given efficiency can be smaller. That is why the rectangular wing or any wing with a high tip lift coefficient is a good candidate for a wing tip drag reducing device (see Ref. 1, paper by Thomas).

By the same reasoning as above, we can see why the addition of a tip device on an optimally loaded CTOL wing will have a relatively smaller (or perhaps no) effect than when placed on a highly loaded tip. If the vortex span is held at $\pi/4$ then an integral scale of the order of 10% of the span would be required to obtain a 20% reduction of the induced drag (Point D in Figure 3.1). The required vertical dimensions of the tip device are much greater than if the load is first distributed onto the tip (e.g. at Point B). The main point is that tip devices will be most effective if they are designed as an integral part of the overall wing design. If one is faced with the problem of retrofitting an existing piece of hardware then it is essential to acquire a knowledge of the bare wing tip load distribution before considering a particular device. Otherwise you can end up with something worse than the bare wing.

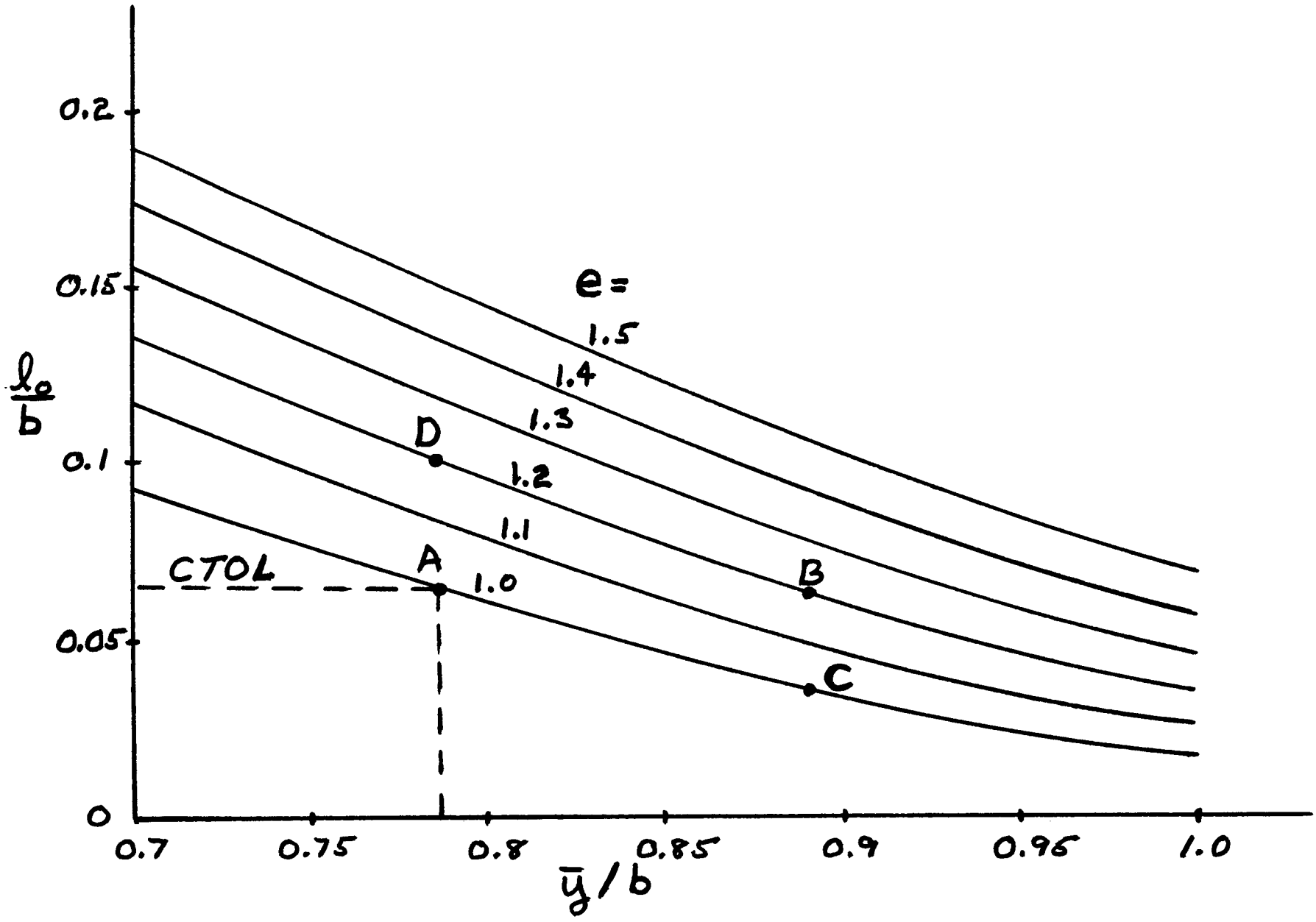

Figure 3.1 - Vortex Wake Integral Scale Versus Vortex Span for Constant Values of Induced Drag Efficiency, (see Eq. 3.2.1).

The most comprehensive recent study of wing tip devices both in-plane and out-of-plane is contained in Ref. 2. Much of what we have discussed above is addressed therein with theoretical calculations and experiment. In terms of wing induced drag efficiency the tip planform is a crucial factor in achieving a good design as we have noted. Efficiencies slightly greater than unity can be achieved with a swept back tip (see Figure 4 of Ref. 2 e.g.) (The parameter χ_{ell} of Ref. 2 is the reciprocal of our factor e). Properly used, wing theory will dictate a good tip shape (see Ref. 11) What is more remarkable is that the swept tip yields an $(L/D)_{max}$ of 22 with an induced drag efficiency of 1.02 (see Figure 27e of Ref. 2) at an aspect value of 7.05. A large soaring bird with tip feathers fully extended has an $(L/D)_{max}$ of about 23 with an induced drag efficiency of 0.87 and aspect ratio of 5 to 6, (Figure 27a of Ref. 2). A wing that has the ability to get a higher maximum L/D without any induced drag penalty is clearly a superior design. The swept tip or feathered tip can maintain a load at higher angle of attack and for soaring or for tip control that is an advantage. It may well be in the area of maximum lift or control performance that most tip devices will prove their superiority over the CTOL wing. Active tip devices might also be considered seriously in the control of fighter type aircraft.

Also in Ref. 2, Figure 20, the author shows three out-of-plane configurations and their induced drag efficiencies. The results are summarized in Figure 3.2. The first point of the example is that large out of plane dimensions are required to realize the maximum benefit of the vorticity diffusion effect. A 20% span vertical end plate does not seem like a practical wing design. Also, the above example illustrates another important point (or question) that must be kept in mind when comparing out-of-plane tip devices to the CTOL wing. A large benefit is calculated for the case of the vertical end plate (42%). However, if the same end plate is used to extend the wing span, an efficiency factor of 1.38 is calculated. In other words turning 20% of the span up on a given wing only yields an efficiency factor e = 1.029 or 2.9% improvement. It would seem more realistic to compare wings on the basis of the length of the load line or wetted area. On the other hand if a particular design is span limited for some reason (e.g., upper bound on root bending moment, fixed keel draft on the 12 meter sailboat hull or fixed span on the 15 meter sailplane) then it does make sense to add vertical devices to increase the lift and drag performance of the original in-plane wing.

In summary, tip devices that are properly designed as an integral part of a wing and not as an add-on have the potential of increasing induced drag efficiency by 10 to 15% when out-of-plane dimensions are of the order of the wing chord. These devices also have great potential for increasing the maximum L/D and high lift performance in particular if they are developed as active devices. In retrofitting existing hardware it is most important to determine the tip loading before considering a tip device. A given device can be detrimental when added on to a good CTOL wing. Finally we remark that the rectangular wing tip can be improved with almost any sensible tip device.

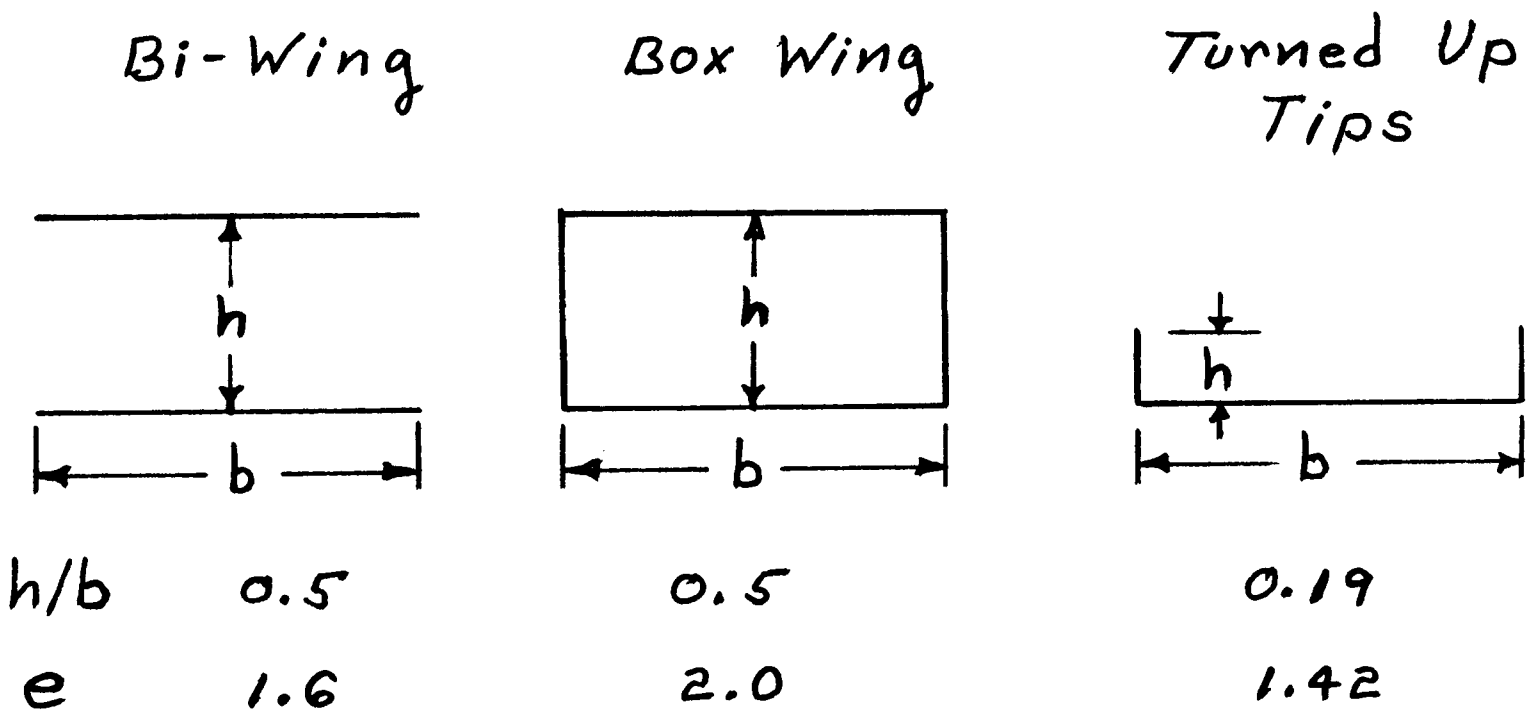

Figure 3.2 - Examples of Out-of-Plane Lifting Configurations (Ref. 2).

3.3 Joined Tip Configurations

The three out-of-plane examples included in the last section (Figure 3.2) illustrate dramatically how drag efficiency can be improved with joined tips (box-wing) or a multi-wing (bi-wing) configuration. This has been known, for many decades (see Hoerner, Ref. 10, e.g.). To implement these devices however, the structural weight and parasite drag penalty has been such as to make their overall performance less than the conventional mono-wing configuration. Recently, there has been a resurgence of interest in the joined tip configuration. According to Ref. 4, NASA Ames and NASA Dryden hope to have the AD-1 aircraft converted and flying with a joined tip configuration within two years. The advantages of this configuration are many fold at least on paper. The primary advantage is the weight reduction that results from the truss like joined wing structure. The weight reduction is of course directly reflected as a reduction of induced drag. The projection of the joined wing on the Trefftz plane also has an induced drag efficiency that is superior to that of the mono-wing. The main purpose of the following discussion is to estimate the maximum practical induced drag benefit that could be expected with a joined wing independent of the structural advantages on disadvantages. We strongly recommend, however, that the integrated (synergistic) structural/aerodynamic design approach be followed in practice (see comments of Wolkovitch in Ref. 4).

For an absolute upper bound on what is attainable in the way of induced drag efficiency the box-wing yields a factor of two when the upper and lower lifting surfaces are separated by haf the span; i.e., $e = 2$ in our formula (3.2.1). Whether this efficiency can be obtained in practice or whether the box wing is a practical design is a separate (and important) issue. The interference drag due to the four corners and whatever wing-fuselage joints are required may be prohibitive. However, we can safely say that "whatever is done", halving the induced drag efficiency of the CTOL wing is a good working upper bound.

To obtain a more practical upper bound we present the results of a minimum induced drag calculation for the joined wing. The result is obtained as follows: Suppose that we consider the class of joined wings that have a continuously turning load line of fixed length when projected on the Trefftz plane. We ask what is the shape of the Trefftz plane projection that minimizes the induced drag and what is the load distribution? The results are presented in Figure 3.3. The shape of the wing as viewed from the Trefftz plane is a flattened elliptical shape with a height of 0.19 of the span. The induced drag efficiency, e, compared to a CTOL wing of span b is 1.25, a 25% improvement. The load distribution varies continuously from the upper to lower wing surface, passing through zero at the tips. The load is essentially elliptic on the upper and lower sections when plotted against distance along the load line.

The above example is only a glimpse of the power of minimum induced drag theory in arriving at optimal joined tip and other configurations. If the ground rules of the minimization process are changed by overall mission requirements then a different configuration will be obtained. The calculated

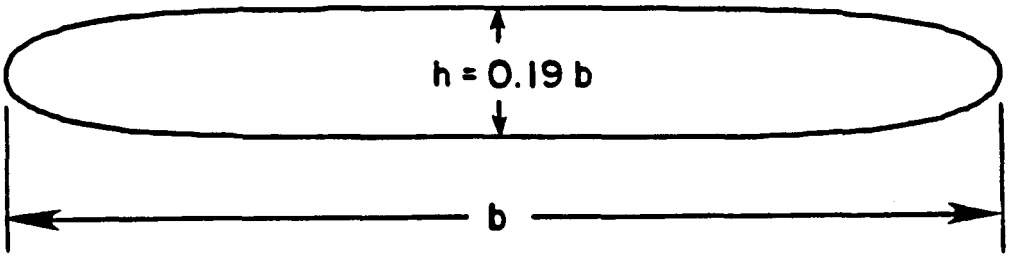

Figure 3.3 - Optimal Joined Tip Wing (Projection on the Trefftz Plane).

25% reduction of induced drag is a good practical estimate of what can be achieved in the way of improved wing efficiency with joined tips. We reiterate that whether a particular minimum drag configuration is structurally practical is a separate and important matter. The aerodynamicist must provide the designer with a variety of choices and the computational tools to rapidly evaluate the drag efficiency of each choice in an integrated design approach.

Final Remarks

In our assessment of drag-due-to-lift reduction devices, we have focused on the advantages and disadvantages of various in-plane and out-of-plane lifting configurations in reducing the theoretical minimum drag. Furthermore, we have stressed the idea that the true drag efficiency of a particular design must be measured against the theoretical minimum. To conclude our discussion, we want to emphasize a point that we have alluded to frequently but have not addressed explicity in our discussion; i.e., that the real wing design problem is to select the planform, section profile, tip shape, etc. to achieve the theoretical minimum.

The computational tools are available for making that selection intelligently (see Ref. 11). Once the Trefftz plane projection of the configuration has been defined, minimum induced drag theory (Refs. 12,13 and 14) will yield the transverse load distribution on all lifting elements. The second step is to use wing theory (potential flow) with the specified span load distribution to determine the approximate planform that can support the required load. Finally, some form of boundary layer theory must be used to determine in detail whether the calculated potential flow and wing section geometry are compatible; i.e., whether the flow remains attached over the entire wing surface subject to the necessary chordwise load variation. The final optimal configuration with respect to total cruise drag will require several iterations between the applications of wing theory and boundary layer theory and finally experiment. All tricks of the trade (e.g., tip shaping, leading edge shaping, trailing edge modifications (including serrations), wash in or wash out and surface treatment can and should be used to achieve a wing efficiency as close as possible to the theoretical maximum. The CTOL wing is an excellent example of design ingenuity (honed by experience) in achieving this goal. The objective in the future should be to optimize the more viable out-of-plane configurations following the same procedures.

4. CONCLUSIONS AND RECOMMENDATIONS

Fundamental relations for the drag and lift of a lifting configuration are derived from the first principles (conservation laws) of fluid mechanics. Many representations (some old and some new) of the fundamental forces are derived in terms of far wake properties, intermediate wake properties and surface loading. The main assumptions that underly the basic theoretical results and conclusions are as follows:

1. There is no mass, momentum or energy exchange at the surface of the lifting configuration. Active drag reduction devices cannot be evaluated with the formulas of this study.

2. The flow Reynolds number is at least 10^6 or greater.

3. All configurations are in steady flight.

4. All configurations are spanwise symmetric.

5. Drag contributions of the order of the square of the drag coefficient (a few counts) are neglected.

The most important conclusions of this study are summarized below:

1. All drag is ultimately of viscous origin and is given by the total head loss or entropy rise in the very far wake (see Eq. (2.2.8)).

2. In the intermediate wake region the drag (and lift) can be expressed quite naturally in terms of vorticity moments and correlations in the Trefftz plane (see Eq. (2.3.21). The first major component of drag is the polar moment of the transverse vorticity that is produced by streamwise variations of the surface load distribution. The second major component is the logarithmic correlation of the axial or streamwise vorticity that is produced by transverse variation of the load distribution.

3. On the surface of the body the drag and lift are given directly in terms of the resultant pressure force and the resultant viscous force (see Eqs. (2.1.2), (2.1.8) and Section 2.4).

4. For a high Reynolds number wing the drag and lift are regular functions of the angle of attack so that the drag coefficient can be expressed in terms of the lift coefficient (see Eq. (2.5.5); i.e.,

$$C_D = C_{D_0} + (K_f + K_i)\, C_L^2 \tag{4.2}$$

Both the form drag (C_{D_0}) and the form drag-due-to-lift (K_f) are functions of Reynolds number and depend strongly on details of the wing section design. The induced drag-due-to-lift (K_i) is relatively independent of Reynolds number and depends primarily on the Trefftz plane profile and

load variation.

5. The form and induced drag-due-to-lift are positive and for a modern "well designed" wing the form component is small (a few percent) compared to the induced component. The theoretical minimum drag-due-to-lift is given by the classical induced drag component for each Trefftz plane profile (e.g. $K_i = 1/\pi A$ for the optial CTOL wing with elliptic load).

6. For high aspect ratio CTOL wings (A>6) the interaction between the form and induced drag-due-to-lift is small of the order of the square of the drag coefficient.

Based on the fundamental theoretical relations for drag we have assessed the advantages and disadvantages of various drag-due-to-lift reducing devices. The conclusions are as follows:

7. CTOL Wings. The well designed modern CTOL wing is nearly optimal with a total drag-due-to-lift within a percent or so of the theoretical minimum. Improvements will be small and are best implemented at the operational level. The profiled wing tip like that on the Boeing 757 accounts for about 0.5% of airplane drag. The CTOL wing alone is not a fruitful configuration for drag-due-to-lift reduction research.

8. Out-of-Plane Tip Devices. Out of plane wing tip devices like winglets, sails and feathers can reduce the drag-due-to-lift of a CTOL wing if the wing and tip device are designed as an integral unit with the proper load distribution on all lifting elements as required by minimum induced drag theory. Highly tip loaded (i.e., improperly designed) CTOL wings are good candidates for retrofitting with tip devices. The performance of a good CTOL wing can be reduced with a tip device. With good outboard loading on the primary wing, a tip device with vertical dimensions of the order of the mean aerodynamic chord can probably achieve a 10 to 15% reduction of the induced drag. Out-of-plane tip devices should definitely be a part of drag-due-to-lift reduction research.

9. Joined-Tip-Configurations. Joined tip configurations offer the possibility of a 25% (or even greater) reductions of drag-due-to-lift without considering the additional potential structural advantages. Investigation of such configurations both aerodynamically and structurally should be given a high priority in current drag-due-to-lift reduction research.

Whether the problem is one of designing a CTOL wing, wing with tip devices or jointed tips the guidelines for obtaining low drag are established and reasonably well understood. We summarize our recommendations for future drag-due-to-lift reduction research in terms of the above single formula (4.1) of this section:

1. Drag-due-to-lift consists of two main parts 1) the classical induced drag (K_i) that depends on the wing span load distribution for the particular Trefftz plane projection and 2) the form drag-due-to-lift (K_f) that

depends primarily on the chordwise load distribution independent of aspect ratio. The first and largest component is more or less independent of Reynolds number while the second component is highly dependent on Reynolds number and details of the wing section design.

2. A fruitful area of drag-due-to-lift reduction research is the following: Based on realistic design scenarios (i.e., bounds on wing lift, span, vertical dimensions, root bending moment, etc.) postulate classes of Trefftz plane configuration and calculate with minimum induced drag theory the optimal configuration and the required load distribution within each class. Define a common rational basis for comparing the induced drag for configuration of the same class and between classes, e.g., use the total wetted area and/or length of load bearing elements in the Trefftz plane. Document these configurations in a systematic way for future design tradeoff studies.

3. A second and follow up area of research would be to use wing load theory (potential theory) in conjunction with boundary layer theory to define the best planform and section profile design for each of the configurations obtained in Step 2. The objective of this step is to minimize the form drag C_{D_0} and profile drag-due-to-lift (K_f) in (4.1).

4. Total airplane drag-due-to-lift reduction is also a profitable area for research. So-called interference drag between airplane components is only another name for unnecessary drag-due-to load variations. The underlying principles summarized in this report are equally valid and relevant for attacking problems of total airplane drag reduction.

5. Finally we reiterate the recommendation in the last paragraph of the introduction. The main assumption of this study is the restricted boundary condition at the surface. The theory of Section 2 must be revised to include mass, momentum and energy exchange. Optimal or even ideal blown configurations or active surface configurations can then be synthesized and current ideas can be evaluated rationally.

REFERENCES

1. Aircraft Drag Prediction and Reduction; presented as a special course at the von Kárman Institute, Rode-St-Genese, Belgium on 20-23 May 1985 and NASA Langley, USA on 5-8 August 1985, AGARD Report No. 723.

2. Zimmer, H., "Die Aerodynamische Optimierung von Tragflugein im Untershall geshwindigkeitsbereich und der Einfluss der Gestaltung der Flugelender," Institut fur Aerodynamik und Gasdynamik Universitat Stuttgart, 1983; (AIAA Tech. Information Service, 555 West 57th St., New York, NY 10019).

3. Whitcomb, R.T., "Methods for Reducing Subsonic Drag-Due-To-Lift," AGARD Report No. 654, p. 2-1, 2-17, Special Course on Concepts for Drag Reduction, von Karman Institute, Rhode-St-Genese, Belgium, 28 March - 1 April 1977.

4. New Tricks for Cutting Drag; ed. Bruce Frisch, Aerospace America, January 1985.

5. Finch, Reg, "Wingtip Design," Sport Aviation, March 1984.

6. Wu, J.M., Vakili, A.D., and Gilliam, F.T., "Aerodynamic Interactions of Wing Tip Flow with Discrete Wingtip Jets," AIAA-84-2206, AIAA 2nd Applied Aerodynamics Conference, August 21-23, 1984, Seattle, Washington.

7. Tarella, D., Wood, N. and Harrits, P., "Measurements on Wing-Tip Blowing," JIAA TR-64, Stanford University, Department of Aeronautics and Astronautics, Stanford, CA, 94305, June, 1985.

8. Betz, A., "Behavior of Vortex Systems," NACA Tech. Memo 713, 1933, (see AIAA Professional Study Series, Vortex Wakes of Large Aircraft under the direction of Coleman duP. Donaldson).

9. Abbott, I.H. and von Doenhoff, A.E., "Theory of Wing Sections," Dover Publications, Inc., New York, NY, 10014, 1985.

10. Hoerner, S.F., "Fluid-Dynamic Drag," Hoerner Fluid Dynamics, (Brick Town, NJ), c.1965.

11. Rubbert, P.E. and Saaris, G.R., "Review and Evaluation of a Three-Dimensional Lifting Potential Flow Analysis Method for Arbitrary Configurations," AIAA Paper No. 72-188, January 1972.

12. Ashenberg, J. and Weihs, D., "Minimum Induced Drag of Wings with Curved Planform," J. Aircraft, January 1984.

13. Cone, C.D., "The Theory of Induced Lift and Minimum Induced Drag of Nonplanar Lifting Sytems," NASA TR-R-139, 1962.

14. Cone, C.D., "The Aerodynamic Design of Wings with Cambered Span Having Minimum Induced Drag," NASA TR R-152, 1963.

1. Report No.	2. Government Accession No.	3. Recipient's Catalog No.
NASA CR-4004		

4. Title and Subtitle	5. Report Date
A Fundamental Study of Drag and an Assessment of Conventional Drag-Due-to-Lift Reduction Devices	September 1986
	6. Performing Organization Code 1A 844

7. Author(s)	8. Performing Organization Report No.
John E. Yates and Coleman duP. Donald	A.R.A.P. Report 577
	10. Work Unit No.

9. Performing Organization Name and Address	11. Contract or Grant No.
Aeronautical Research Associates of Princeton, Inc. 50 Washington Road, P.O. Box 2229 Princeton, New Jersey 08543	NAS1-18065
	13. Type of Report and Period Covered
12. Sponsoring Agency Name and Address National Aeronautics and Space Administration Washington, DC 20546	Contractor Report
	14. Sponsoring Agency Code 505-60-31

15. Supplementary Notes

Langley Technical Monitor: Floyd G. Howard

16. Abstract

The integral conservation laws of fluid mechanics are used to assess the drag efficiency of lifting wings, both CTOL and various out-of-plane configurations. The drag-due-to-lift is separated into two major components: 1) the "induced" drag-due-to-lift that depends on aspect ratio but is relatively indepentent of Reynolds number. 2) the "form" drag-due-to-lift that is independent of aspect ratio but dependent on the details of the wing section design, planform and Reynolds number. For each lifting configuration there is an optimal load distribution that yields the minimum value of drag-due-to-lift. For well designed high aspect ratio CTOL wings the two drag components are independent. With modern design technology CTOL wings can be (and usually are) designed with a drag-due-to-lift efficiency close to unity. Wing tip-devices (winglets, feathers, sails, etc.) can improve drag-due-to-lift efficiency by 10 to 15% if they are designed as an integral part of the wing. As add-on devices they can be detrimental. It is estimated that 25% improvements of wing drag-due-to-lift efficiency can be obtained with joined tip configurations and vertically separated lifting elements without considering additional benefits that might be realized by improved structural efficiency. It is strongly recommended that an integrated aerodynamic/structural approach be taken in the design of (or research on) future out-of-plane configurations.

17. Key Words (Suggested by Author(s))	18. Distribution Statement
Drag Lift Drag Reduction Vorticity	Unclassified - Unlimited Subject Category 34

19. Security Classif. (of this report)	20. Security Classif. (of this page)	21. No. of Pages	22. Price
Unclassified	Unclassified	54	A04

For sale by the National Technical Information Service, Springfield, Virginia 22161

NASA-Langley, 1986